

## Models of slow rotational mobility of paramagnetic probes in glassy media

A. Kh. Vorob'ev,\* V. S. Gurman, and T. A. Klimenko

Department of Chemistry, M. V. Lomonosov Moscow State University,  
Leninskie Gory, 119899 Moscow, Russian Federation.  
Fax: +7 (095) 932 8846. E-mail: vorobiev@excite.chem.msu.ru

Experimental ESR spectra of the 2,2,6,6-tetramethyl-4-oxopiperidinoxyl (TEMPO) radical probe in the glycerol, polystyrene, and polyvinylbutyral matrices measured in the temperature range 77–373 K were quantitatively compared with the ESR spectra calculated using the known theoretical models of rotational mobility. It was shown that simulation of ESR spectra by the nonlinear least-squares method is an efficient procedure for discriminating between theoretical models. The temperature ranges were determined in which it is possible to achieve quantitative agreement between experimental and theoretical spectra as well as the ranges in which theoretical models are insufficient to quantitatively describe the experimental results. It was established that the widely used model of Brownian diffusion in isotropic medium is inadequate to describe the ESR spectra in the case of slow motions of small probe molecules. It was found that specific interactions (formation of weak complexes) between the probe molecules and the molecules of the medium results in strongly anisotropic molecular rotational motions.

**Key words:** ESR spectroscopy, radical probes, nitroxyl radicals, molecular mobility, simulation of ESR spectra by the nonlinear least-squares method, glassy media, glycerol, polystyrene, polyvinylbutyral.

The method of paramagnetic probe is widely used for studying the molecular dynamics in various media, *e.g.*, isotropic liquids,<sup>1,2</sup> liquid crystals,<sup>3</sup> biological objects,<sup>4</sup> and polymers.<sup>5–8</sup> It is based on comparison of experimental and simulated ESR spectra of paramagnetic probes (usually, nitroxyl radicals). The method makes it possible to judge not only the characteristic rotational correlation times ( $\tau_c$ ), but also the types of elementary motions, molecular ordering, and other microscopic details of the process under study.<sup>9</sup>

Recent studies on quantitative simulation of ESR spectra have shown that a good correspondence between the simulated and experimental spectra is observed in the region of fast rotational motions ( $\tau_c < 10^{-9}$  s). Data on the rotational correlation times obtained in these studies are in good agreement with the results of rotational mobility measurements by the dielectric relaxation method and NMR spectroscopy.

Simulation of ESR spectra in the region of slow motions is much more complicated. No good quantitative agreement between experimental and simulated spectra is usually observed in this case.

In the region of slow motions, the results of the studies carried out by the method of paramagnetic probe differ from those obtained using other physical methods by several orders of magnitude.<sup>7,8</sup> These discrepancies are usually explained assuming that different methods are sensitive to different types of motions. However, no convincing arguments supporting this viewpoint have been adduced.

For long, the mechanisms of rotational motions of probes have been described using the models of Brownian diffusion or jump diffusion in isotropic medium.<sup>9</sup> Incompleteness and inadequacy of the concepts of isotropic medium became obvious after obtaining new experimental data. Using the spin echo and saturation transfer methods, the high-frequency, small-amplitude vibrations (librations) of paramagnetic probes in glassy media were detected. Librational motions of nitroxyl radicals with characteristic times of  $10^{-9}$ – $10^{-11}$  s and amplitudes of at most  $10^\circ$  were detected both in polymers<sup>10,11</sup> and in low-molecular weight matrices.<sup>12,13</sup> In conventional ESR spectra, librations manifest themselves as a weak linear temperature dependence of effective magnetic parameters.<sup>14,15</sup>

Previously,<sup>16</sup> we have shown that the molecules of nitroxyl probes placed in polymer matrices and oriented by irradiation with polarized light lose their orientation (*i.e.*, rotate) at  $T = 200$ – $300$  K with correlation times of the order of minutes. A rather strong temperature dependence of the ESR spectra of the probes is also observed in the same temperature range. Previously, it was explained by rotation of the molecules with  $\tau_c \sim 10^{-7}$  s. Thus, the results obtained by different methods are contradictory. After analysis of this contradiction it was inferred that the environment of the probe molecule in the polymer matrix is highly anisotropic.

These considerations, as well as some other experimental observations<sup>11–14</sup> prompted us to discuss the rotational mobility in terms of the concept of a "cage"

containing an impurity molecule in a glassy medium (e.g., polymer) rather than models of isotropic medium. Among the models of rotation of a guest molecule in the solvent cage, the model of slowly relaxing local structure (SRLS)<sup>17</sup> is characterized by the highest level of generalization. This model considers the motion of the probe molecule as reorientation in the mobile anisotropically shaped solvent cage. The cage itself rotates in the course of its reorganization and its tensor of the rotational diffusion coefficient differs from that of the probe molecule. The effect of the cage on the probe rotation is taken into account by introducing the interaction potential in which the probe moves (the cage potential). Thus, in the framework of the SRLS model the motion of the probe can be considered as a motion of two coupled rotors. The model has been tested in the simulation of high-resolution ESR spectra (250 GHz) of nitroxyl radicals in low-molecular weight glasses and supercooled liquids<sup>17-19</sup> and in liquid-crystalline side-group polymers.<sup>20</sup> The drawbacks of the model are a large number of parameters and the problems associated with the software implementation of the simulation program. To date, calculations using this model have only been carried out for the axially symmetric matrix cage and rotating probe.<sup>17</sup>

Most of the other rotational mobility models can be considered as particular (simpler) cases of the SRLS model. The MOMD (microscopic order — macroscopic disorder) model<sup>21,22</sup> uses the potential generated by the anisotropic cage in which the probe molecule moves; however, the matrix cage is assumed to be immobile. Currently, the MOMD model is used more often than the SRLS model because of much simpler numerical implementation.

The model of librations can be considered as a particular case of the SRLS and MOMD models where the height of the potential barrier produced by the matrix cage is much higher than the thermal energy,  $kT$ . In this case, rotational motions of the probe are small-angle displacements from the equilibrium position near the potential minimum. These features are characteristic of crystalline matrices and glassy media at low temperatures. Previously,<sup>16</sup> a temperature range was shown to exist for glassy polymers at temperatures below their glass transition temperatures ( $T_g$ ), in which rotational motions of the probe in the matrix cage are characterized not only by large amplitude (up to  $15^\circ$ ), but also by high frequency motions (i.e., they are averaging motions in the ESR frequency scale). In order to distinguish between these motions and true harmonic librations, we will call them quasibrations. If only librations and quasibrations manifest themselves in an ESR spectrum, its pattern corresponds to that of the ESR spectrum of a fixed species, whose effective magnetic parameters are changed due to high-frequency motions. In this approximation, the temperature range suitable for simulation of ESR spectra depends on the operating frequency of the ESR spectrometer.

Up to now, slow rotation of probe molecules in amorphous glassy polymers was mostly considered in the framework of the model of Brownian motion in isotropic medium.<sup>23,24</sup> The rotational correlation times were assessed from the separation between the outermost extrema of the ESR spectrum of a nitroxyl radical. The results of simulation of the ESR spectral patterns of radical probes were for the most part estimated using a qualitative (visual) comparison of the simulated and experimental spectra. These simulations were aimed at reproducing only the splittings between the spectral components. Such an approach seems to be oversimplified. The nonlinear least squares method (LSM) used in several recent studies<sup>15-18,20</sup> provides much more rigorous criteria for correspondence between simulation and experiment.

In the context of the aforesaid, of considerable importance is to revise at a new quantitative level the patterns of the ESR spectra of nitroxyl probes in glassy and, especially, in polymer matrices at temperatures below  $T_g$  and to determine the limits of applicability of the known models of rotational mobility to description and prediction of experimental results.

The disordered media used in this work were glycerol (a low-molecular weight glassy matrix), polystyrene, and polyvinylbutyral, the last two compounds being representatives of wide classes of glassy polymers with high glass transition temperatures. 2,2,6,6-Tetramethyl-4-oxopiperidinoxyl (TEMPO), which is one of the most widely used nitroxyl radicals, was used as paramagnetic probe.

## Experimental

The samples used were TEMPO-containing polystyrene films cast on a cellophane substrate from a solution of TEMPO and polystyrene in benzene, dried in air until solidification, and then evacuated *in vacuo* ( $\sim 10^{-3}$  Torr) for 24 h. The thickness of the films was  $\sim 200$   $\mu\text{m}$  and the concentration of TEMPO was  $2 \cdot 10^{-3}$  mol L<sup>-1</sup>. Polyvinylbutyral films were prepared analogously using chloroform as solvent. To eliminate the effect of oxygen on the pattern of the ESR spectrum, samples placed in quartz ampoules were evacuated *in vacuo* ( $\sim 10^{-3}$  Torr) for 6 h.

Samples of TEMPO in glycerol (the content of water was less than 0.5%) were prepared by dissolving the desired amount of radical in glycerol.

The ESR spectra of evacuated samples were recorded on a Varian E-3 spectrometer in the 3-cm wave band. The desired temperature in the range between 77 and 473 K was maintained using a temperature accessory to the Varian E-3 ESR spectrometer with an accuracy of  $\pm 2^\circ$ . It was established that it takes no longer than 100 s for the polymer films and glassy samples to take on the specified temperature.

## Procedure for simulation of ESR spectra

Experimental ESR spectra were simulated using the nonlinear LSM. The best fit parameters used to describe the experimental pattern of the ESR spectrum were

found by minimizing the sum of the squares of the deviations of the simulated spectra from experimental ones in the parameter space using an adaptive procedure.<sup>25,26</sup> The simulation was considered adequate, and the corresponding set of parameters was taken as providing the best fit, if the sum of the squares of the deviations of the simulated spectrum from the experimental one, divided by the number of points in the simulated spectrum, did not exceed  $1.5 \cdot 10^{-5}$ . This value was chosen so that it can approximately correspond to the noise amplitude in the experimental spectrum. Experimental ESR spectra (the magnetic field sweep in G) were preliminarily normalized to the value of their double integral. Otherwise, the correspondence between the simulated and experimental spectra becomes worse. Dispersions of the best fit parameters were calculated using the corresponding elements of the covariation matrix at the minimum point. It was verified that the correspondence between the simulated and experimental spectra is retained if the orientations of the axes of the  $g$ -tensors and HFC tensors differ within  $5^\circ$ .

The ESR spectra of fixed species were simulated in the high-field approximation. Our preliminary studies showed that the spectra simulated in this approximation virtually coincide with those obtained using the complete simulation procedure. A known<sup>27</sup> set of parameters (the components of the  $g$ -tensor and HFC tensor and the width of individual line) was used as initial approximation. The magnetic parameters of the radical, varied in the course of minimization were the components of the  $g$ -tensor and HFC tensor, as well as the parameters describing the shape of individual lines. Calculations were performed using the convolution of the Lorentz and Gaussian functions to describe the shape of individual lines. For each function, the halfwidth could be set as a tensor whose axes were directed parallel to those of the  $g$ -tensor.

The minimization procedure converged to the same minimum if the initial set of parameters was within the physically substantiated limits. The set of the best fit parameters obtained after such an optimization includes the effective components of the  $g$ -tensor and HFC tensor averaged by fast small-amplitude rotational motions, *i.e.* it corresponds to the models of librations and quasibrations. Average angular displacements corresponding to restricted rotational motions considered in the model of quasibrations can be found as the solution of the system of equations<sup>16</sup> using the effective magnetic parameters:

$$\begin{aligned} \bar{A}_x &= A_x + (A_z - A_y)S_y + (A_y - A_z)S_z, \\ \bar{A}_y &= A_y + (A_z - A_x)S_x + (A_x - A_z)S_z, \\ \bar{A}_z &= A_z + (A_y - A_x)S_x + (A_x - A_y)S_y, \end{aligned} \quad (1)$$

where  $\bar{A}_x$ ,  $\bar{A}_y$ , and  $\bar{A}_z$  are the effective (averaged) components of the HFC tensor,

$$\begin{aligned} S_x &= \langle \sin^2 \alpha_x \rangle, \\ S_y &= \langle \sin^2 \alpha_y \rangle, \\ S_z &= \langle \sin^2 \alpha_z \rangle, \end{aligned}$$

where  $\alpha_x$ ,  $\alpha_y$ , and  $\alpha_z$  are the angles of rotational displacements about the  $x$ ,  $y$ , and  $z$  axes, respectively; and the angular brackets denote the averaging over the ensemble. A system of equations analogous to system (1) is also valid for the effective components of the  $g$ -tensor. However, these values can be calculated more reliably and in a shorter time if the minimization procedure makes it possible to vary the  $\langle \sin^2 \alpha_x \rangle$ ,  $\langle \sin^2 \alpha_y \rangle$ , and  $\langle \sin^2 \alpha_z \rangle$  values simultaneously and if the magnetic parameters are obtained using formulas (1). It is these calculations that were used to obtain the results discussed below.

The ESR spectra of radical probes rotating in an isotropic medium were simulated using Freed's simulation program (Version 1.6)<sup>29</sup> with fixed magnetic parameters equal to those obtained at 77 K. We varied dynamic parameters, namely, the correlation times, orientations of the axes of rotation, and the parameters characterizing the shape of individual lines. As a rule, the minimization procedure converged to the only global minimum.

In addition to the models of rotational diffusion in isotropic medium, the MOMD model was also used. It was found that simulation performed using simultaneous involvement of the rotational correlation times and parameters of the potential exerted to the rotating species in the variation procedure leads to a rather large number of approximately equally deep minima with strongly different best fit parameters. Such ambiguity of the simulation procedure indicates that the experimental spectrum can be simulated with nearly the same quality using different sets of parameters of the model.

It should be noted that the minimization procedure for the sum of the squares of the deviation of the simulated spectrum from experimental one is much more "sensitive" to the choice of the model of motion than the simulation of spectra with visual control or the reproduction of particular spectral characteristics such as positions of peaks, halfwidths of lines, *etc.* Simulated spectra qualitatively similar to the experimental spectra can be obtained using different models of motion. However, often the set of parameters obtained using visual control does not correspond to the minimum of the sum of the squares of deviations and, moreover, visual similarity with experimental results is impaired as the system approaches this minimum. This indicates an incorrect choice of the model. In some instances, the use of another model of motion made it possible to obtain excellent agreement between simulated and experimental spectra.

## Results of simulation

### Determination of the principal values of magnetic parameters

Table I lists the principal values of the  $g$ -tensors and HFC tensors of the TEMPON radical in the glycerol,

polystyrene, and polyvinylbutyral matrices obtained by optimizing the ESR spectra in the region of completely hindered rotational motion (the "rigid limit"). Optimization of the ESR spectra of the TEMPON radical in polymer matrices at 77 K (for the glycerol matrix, at 113 K) was performed so that the  $\bar{g}$ -values remained unchanged and equal to those reported in the literature. For some reasons (see below), we failed to obtain a satisfactory correspondence between the simulated and experimental ESR spectrum of the probe in the glycerol matrix at 77 K. The values of magnetic parameters taken from the literature are also listed in Table 1. As can be seen, the components of the  $g$ -tensor of the TEMPON radical in the polystyrene matrix in the presence of oxygen are in good agreement with the reported data.<sup>28</sup> The magnetic parameters of TEMPON in the glycerol matrix appeared to be close to those reported for the deuterated radical in the glycerol- $d_8(85\%)$ - $D_2O$  mixture.<sup>30</sup>

It also follows from Table 1 that oxygen, as well as an increase in the polarity of the medium, affects the values of magnetic parameters. Both these factors cause an increase in the  $A_z$  and a decrease in the  $g_x$  value, which is in agreement with the reported data.<sup>27</sup>

Further, the principal values of the magnetic parameters of the TEMPON radical listed in Table 1 were used in the simulation of its ESR spectra at different temperatures.

### Temperature dependence of ESR spectra

Experimental spectra of the TEMPON radical in the glycerol matrix were recorded in the temperature range  $77 < T < 343$  K, which covers the motional regions from the region of "rigid limit" to that of fast rotational motions. The results of simulation of the ESR spectra in the glycerol matrix at different temperatures are presented in Fig. 1. It is convenient to divide the whole temperature range into five intervals (see Fig. 1).

We failed to obtain a satisfactory correspondence between simulated and experimental ESR spectra in the temperature range I near 77 K (see Fig. 1).

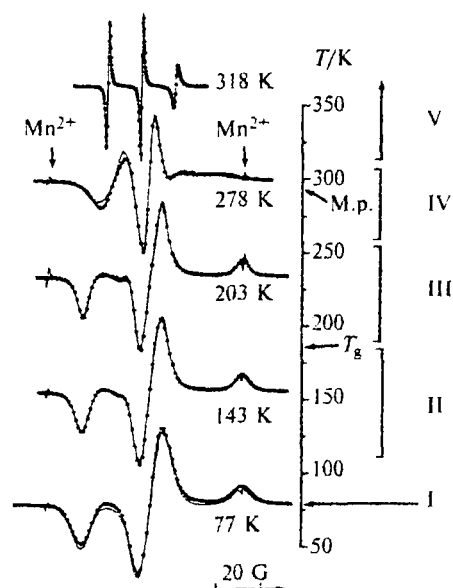


Fig. 1. Results of the best fit simulation of the ESR spectra of TEMPON radicals in glycerol at different temperatures. Solid lines denote the experimental spectra and the points denote the simulated spectra. The temperature ranges of applicability of different models (see text) are indicated at the right.

In the temperature range II (between 113 and 183 K), the experimental spectra can be described well in the framework of the model of fixed species if only the halfwidths of the Gaussian and Lorentz functions ( $\delta_G$  and  $\delta_L$ , respectively) are varied and the values of magnetic parameters remain unchanged. The contribution of the Gaussian function to the pattern of the ESR spectrum decreases as the temperature increases; correspondingly, the contribution of the Lorentz function increases (Table 2). At 183 K, both functions make approximately equal contributions to the spectral pattern.

In the temperature range III (between 183 and 253 K), we failed to describe the ESR spectra satisfactorily by varying the halfwidths of individual lines only. Here, we succeeded in simulating the ESR spectra in the

Table 1. Magnetic parameters of the ESR spectrum of TEMPON radical obtained from simulation of the spectra at the "rigid limit" temperature

| Matrix                                | T/K | $g_i$                         |                               |         | A/G             |                |                  |
|---------------------------------------|-----|-------------------------------|-------------------------------|---------|-----------------|----------------|------------------|
|                                       |     | x                             | y                             | z       | x               | y              | z                |
| Glycerol                              | 113 | $2.00876 \pm 1 \cdot 10^{-4}$ | $2.00645 \pm 1 \cdot 10^{-4}$ | 2.00239 | $5.42 \pm 0.25$ | $3.4 \pm 0.4$  | $35.4 \pm 0.1$   |
| Polystyrene, evacuated sample         | 77  | $2.00937 \pm 5 \cdot 10^{-5}$ | $2.00621 \pm 5 \cdot 10^{-5}$ | 2.00191 | $6.0 \pm 0.2$   | $3.6 \pm 0.3$  | $33.01 \pm 0.08$ |
| Polystyrene, oxygen-containing sample | 77  | $2.00897 \pm 4 \cdot 10^{-5}$ | $2.00632 \pm 4 \cdot 10^{-5}$ | 2.00220 | $6.17 \pm 0.15$ | $4.1 \pm 0.22$ | $32.49 \pm 0.07$ |
| Polyvinylbutyral                      | 77  | $2.00953 \pm 1 \cdot 10^{-4}$ | $2.00599 \pm 1 \cdot 10^{-4}$ | 2.00199 | $5.68 \pm 0.25$ | $3.3 \pm 0.38$ | $34.0 \pm 0.09$  |
| Polystyrene*                          | 77  | 2.0089                        | 2.0062                        | 2.0024  |                 |                | 31               |
| Glycerol- $d_8$ - $D_2O$ mixture**    | 133 | 2.0084                        | 2.0060                        | 2.0022  | 5.5             | 5.7            | 35.8             |

\* Ref.<sup>28</sup>

\*\* Ref.<sup>30</sup>

**Table 2.** Temperature dependence of the parameters of the ESR spectrum of TEMPO radical calculated using the model of quasibrations

| T/K              | $\delta/G$ |     | $\bar{g}$ |         |         | $\bar{A}/G$ |     |       |
|------------------|------------|-----|-----------|---------|---------|-------------|-----|-------|
|                  | G          | L   | x         | y       | z       | x           | y   | z     |
| Glycerol         |            |     |           |         |         |             |     |       |
| 113              | 6.7        | 1.5 | 2.00876   | 2.00646 | 2.00239 | 5.4         | 3.4 | 35.4  |
| 123              | 5.9        | 1.9 | 2.00876   | 2.00646 | 2.00239 | 5.4         | 3.4 | 35.4  |
| 143              | 4.7        | 2.3 | 2.00876   | 2.00646 | 2.00239 | 5.4         | 3.4 | 35.4  |
| 163              | 3.6        | 2.6 | 2.00876   | 2.00646 | 2.00239 | 5.4         | 3.4 | 35.4  |
| 183              | 2.9        | 2.7 | 2.00876   | 2.00646 | 2.00239 | 5.4         | 3.4 | 35.4  |
| 193              | 2.9        | 2.6 | 2.00872   | 2.00646 | 2.00242 | 5.6         | 3.4 | 35.3  |
| 203              | 2.9        | 2.6 | 2.00869   | 2.00647 | 2.00244 | 5.6         | 3.4 | 35.2  |
| 213              | 2.7        | 2.6 | 2.00866   | 2.00647 | 2.00247 | 5.8         | 3.4 | 35.0  |
| 223              | 2.8        | 2.5 | 2.00862   | 2.00648 | 2.00249 | 5.9         | 3.4 | 34.9  |
| 233              | 3.1        | 2.3 | 2.00849   | 2.00655 | 2.00256 | 6.1         | 3.5 | 34.6  |
| 243              | 3.9        | 1.8 | 2.00821   | 2.00667 | 2.00273 | 6.8         | 3.6 | 33.8  |
| 253              | 4.4        | 1.5 | 2.00792   | 2.00685 | 2.00284 | 7.2         | 3.7 | 33.3  |
| Polystyrene      |            |     |           |         |         |             |     |       |
| 77               | 5.4        | 1.6 | 2.00937   | 2.00621 | 2.00191 | 6.0         | 3.6 | 33.0  |
| 113              | 4.5        | 1.7 | 2.00906   | 2.00645 | 2.00199 | 6.1         | 3.8 | 32.7  |
| 133              | 4.4        | 1.3 | 2.00875   | 2.00665 | 2.00210 | 6.4         | 4.0 | 32.3  |
| 143              | 4.3        | 1.2 | 2.00867   | 2.00668 | 2.00215 | 6.5         | 4.0 | 32.15 |
| 153              | 4.45       | 1.0 | 2.00843   | 2.00678 | 2.00229 | 6.9         | 4.1 | 31.6  |
| 163              | 4.3        | 0.9 | 2.00825   | 2.00678 | 2.00248 | 7.6         | 4.1 | 30.1  |
| Polyvinylbutyral |            |     |           |         |         |             |     |       |
| 77               | 7.2        | 1.5 | 2.00953   | 2.00599 | 2.00199 | 5.7         | 3.3 | 34.0  |
| 123              | 4.7        | 2.3 | 2.00903   | 2.00646 | 2.00201 | 5.4         | 3.6 | 33.9  |
| 133              | 4.4        | 2.2 | 2.00889   | 2.00655 | 2.00206 | 5.6         | 3.7 | 33.7  |
| 143              | 4.2        | 2.2 | 2.00882   | 2.00660 | 2.00207 | 5.6         | 3.7 | 33.7  |
| 153              | 3.7        | 2.4 | 2.00869   | 2.00669 | 2.00212 | 5.7         | 3.8 | 33.5  |
| 163              | 4.0        | 2.1 | 2.00866   | 2.00667 | 2.00218 | 6.0         | 3.8 | 33.3  |
| 173              | 3.8        | 2.2 | 2.00855   | 2.00670 | 2.00226 | 6.2         | 3.8 | 33.0  |

Note. Dispersions of the parameters listed in table were no greater than 0.3 G for the halfwidths of the Gaussian ( $\delta_G$ ) and Lorentz ( $\delta_L$ ) lines;  $5 \cdot 10^{-5}$  for  $\bar{g}_x$ ,  $\bar{g}_y$ , and  $\bar{g}_z$ ; and 0.1 G for  $\bar{A}_x$ ,  $\bar{A}_y$ , and  $\bar{A}_z$ .

framework of the model of quasibrations assuming that large-amplitude, high-frequency vibrations of the probe molecules occur, thus causing averaging of effective magnetic parameters.

Our attempts to simulate the experimental ESR spectra using the model of quasibrations or models of diffusion in isotropic medium in the temperature interval IV ( $253 < T < 303$  K) failed. The spectra simulated using the MOMD model are qualitatively similar to the experimental spectra; however, no quantitative agreement was obtained in this temperature range (Fig. 2). When varying the rotational correlation times and parameters of the cage potential, the minimization procedure for the sum of the squares of deviations leads to different minima depending on the choice of initial set of parameters. The reliability and physical meaning of the best fit parameters obtained will be discussed below.

Temperature range V ( $T > 303$  K) corresponds to the region of fast rotational motions ( $\tau_c < 1 \cdot 10^{-9}$  s). In this temperature interval, it is possible to describe the experi-

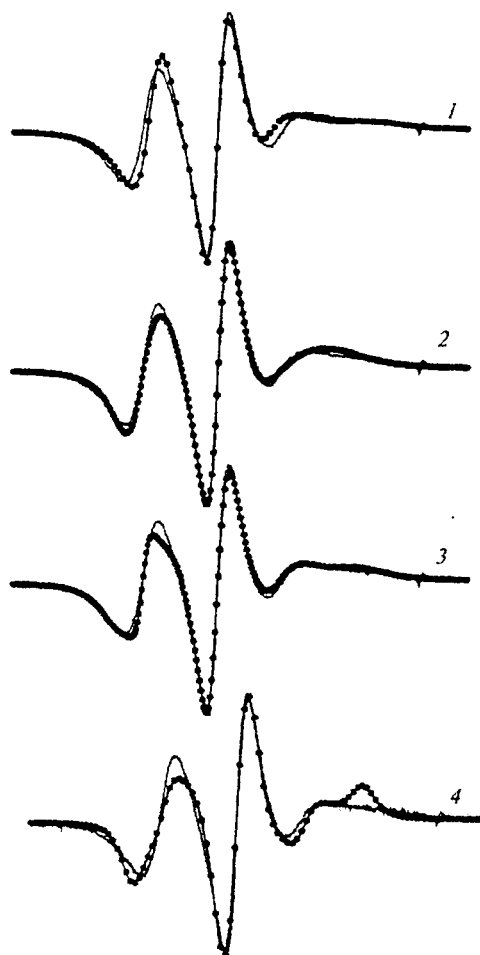


**Fig. 2.** Results of simulation of the ESR spectrum of TEMPO radical in glycerol matrix at 283 K using different models. Solid lines denote the experimental spectrum and points denote the simulated spectrum: the model of Brownian diffusion, the components of the tensor of rotational diffusion  $R_x = R_y = R_z$  (1); the model of Brownian diffusion, the components of the tensor of rotational diffusion  $R_x \ll R_y, R_z$  (2); the MOMD model (3); and the model of quasibrations (4).

mental spectra in the framework of the model of Brownian diffusion in isotropic medium.

Unlike the glycerol matrix, only three qualitatively different temperature intervals can be distinguished in the polymer matrices (Fig. 3). The model of quasibrations satisfactorily describes the experimental ESR spectra in the temperature intervals from 77 to 163 K for polystyrene matrix and from 77 to 173 K for polyvinylbutyral matrix. None of the models used gives quantitative agreement with the experiment in the temperature range  $163 < T < 333$  K. At  $T > 60$  °C, the best fit results for both polymer matrices are obtained by simulating the spectra using the model of motion in isotropic medium with strongly different correlation times for rotational motions about the x, y, and z axes (see Fig. 3).

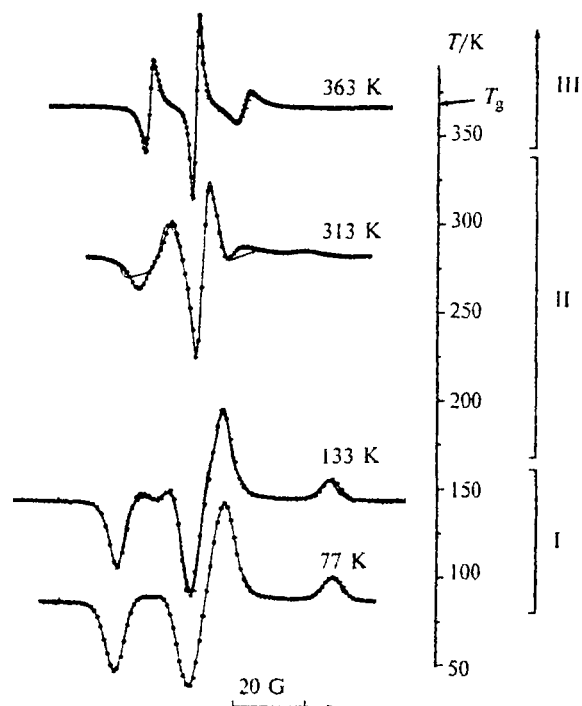


Fig. 3. Examples of the best fit simulation of the ESR spectra of TEMPO radical in polystyrene at different temperatures. Solid lines denote the experimental spectrum and points denote the simulated spectrum. The temperature ranges of applicability of different models (see text) are indicated on the right.

## Results and Discussion

The temperature dependence of the ESR spectra of the TEMPO radical probe in the glycerol matrix appeared to be the most intriguing and complicated among all systems studied in this work. Let us consider the above-mentioned temperature intervals in detail (see Fig. 1).

At 77 K (temperature range I), none of the models used makes it possible to reproduce quantitatively the experimental ESR spectrum. This can be explained by the fact that different sub-ensembles of the probe molecules are characterized by different values of magnetic parameters. It is known that magnetic parameters of nitroxyl radicals differ to some extent depending on the molecular conformation (a chair or a boat), frequency of intramolecular rotational motions of the Me groups, and specific features of the solvation shell, in particular, on the presence of hydrogen bonds with the solvent molecules. If the frequencies of transitions between different states of the radicals are not too high, the ESR spectrum is a superposition of the spectra of the radicals in these states. Such an inhomogeneously broadened spectrum cannot be described using the same set of parameters. Inhomogeneous broadening of the ESR spectrum at 77 K indicates that the glycerol matrix is more rigid than

other polymer matrices studied in this work, for which the ESR spectra of the probe at the same temperature can be simulated satisfactorily. Our experiments show that the frequency of transitions from one to the other molecular sub-ensemble owing to intramolecular motions and small-amplitude molecular motions becomes high enough for satisfactory description of the ESR spectrum as the temperature increases slightly (to 113 K), though the spectrum remains inhomogeneously broadened (the halfwidth of the Gaussian line is  $\sim 6.5$  G).

At  $113 < T < 183$  K (temperature range II), the magnetic parameters remain unchanged. A decrease in the contribution of the Gaussian function to the shape of individual lines suggests that inhomogeneous broadening decreases successively as temperature increases. This indicates unfreezing of small-scale motions. Recently,<sup>15</sup> a weak temperature dependence was found of the magnetic parameters of the deuterated TEMPO radical in a glycerol–water mixture, which was explained by librations with amplitudes no larger than  $6^\circ$ . Changes in the magnitudes of magnetic parameters reported previously<sup>15</sup> lie within the limits of experimental errors of our study because of much greater linewidths of the ESR spectrum of the undeuterated probe. Thus, only small-amplitude motions, in particular, librations, may be thought of as characteristic of temperature range II.

In temperature range III ( $183 < T < 253$  K), the pattern of the ESR spectrum of the probe remains similar to that of the spectrum of fixed radical. However, beginning with  $T = 193$  K, the effective magnetic parameters exhibit a rather strong temperature dependence (see Table 2). It should be noted that these temperatures are higher than the  $T_g$  of glycerol (190–193 K<sup>31</sup>). Recent study<sup>15</sup> of deuterated TEMPO radical in the glycerol- $d_3$ (85%)– $D_2O$  mixture revealed that the temperatures dependence of effective magnetic parameters deviates rapidly in the same temperature range from the linear dependence observed at lower temperatures and typical of librations. Variations of magnitudes of the magnetic parameters indicate that quasibrations, *i.e.*, high-frequency stochastic rotational motions of the species near their equilibrium positions characterized by retention of the equilibrium positions in the time scale of the ESR sensitivity, have a rather large amplitude. Hence in temperature range III the pattern of the ESR spectrum is determined by quasibrations. Recently,<sup>16</sup> we have shown that from variations of the magnitudes of magnetic parameters it is possible to find the amplitude characteristics of such motions, namely, the  $\langle \sin^2 \alpha_x \rangle$ ,  $\langle \sin^2 \alpha_y \rangle$ , and  $\langle \sin^2 \alpha_z \rangle$  values, where  $\alpha_x$ ,  $\alpha_y$ ,  $\alpha_z$  are the angles of rotational displacements about the  $x$ ,  $y$ , and  $z$  magnetic axes, respectively, and the angular brackets denote averaging over the ensemble. The temperature dependences of these characteristics are shown in Fig. 4. As can be seen, in temperature interval II the magnitudes of angular displacements are close to zero. In temperature range III, an increase in the amplitudes of quasibrations about the  $y$  and  $z$  axes is observed and the largest angles

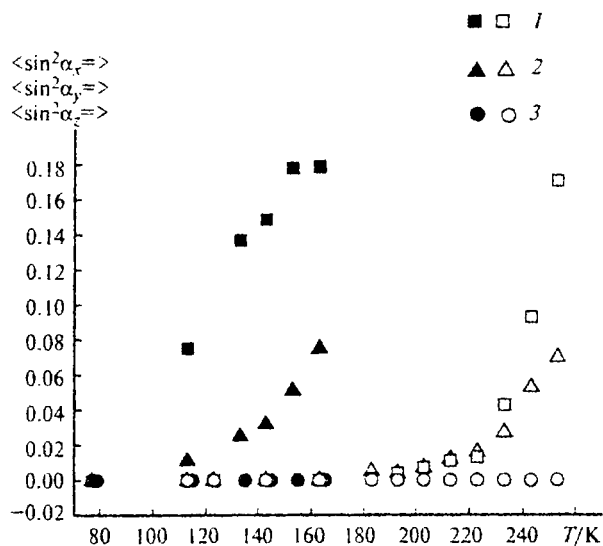


Fig. 4. Temperature dependence of the root-mean-square angular displacements about the  $x$  (1),  $y$  (2), and  $z$  (3) axes obtained using the model of quasibrations. Open and filled circles correspond to glycerol and polystyrene, respectively.

of corresponding rotational displacements are respectively  $15^\circ$  and about  $25^\circ$  at 253 K. Noteworthy is the fact that almost no angular displacements occur about the  $x$  axis directed along the axis of the N—O bond. These marked differences between the possibilities for angular displacements about different axes of the radical to occur are by no means associated with its molecular structure. Explanation for such anisotropic behavior should likely be searched for among peculiarities of intermolecular interactions between the probe and the medium, *i.e.*, of the formation of a weak complex. In this case, the motion about the  $z$  molecular axis, parallel to the axis of p-orbital, will bear a much closer resemblance to free motion than that about the  $y$  (and, especially,  $x$ ) molecular axis of the probe.

Temperature range IV ( $253 < T < 303$  K) is characterized by the strongest temperature dependence of the pattern of ESR spectra of the probe. Qualitatively, it is these changes in the spectral pattern that are expected as rotational mobility of the probe increases. However, we failed to perform quantitative simulation of experimental spectra in this temperature interval using both the model of quasibrations and the model of rotation in isotropic medium (see Fig. 3). We believe that the use of the MOMD and SRLS models for simulating the ESR spectra in this temperature interval seems to be the most physically substantiated. However, our attempt to use the MOMD model failed. The simulated spectra obtained after minimization differ appreciably from the experimental spectra both quantitatively and qualita-

tively. Location of several minima on the hypersurface of the sum of the squares of deviations in the parameter space makes the results of simulation ambiguous. Physical pictures corresponding to different minima differ significantly; at the same time, it is impossible to choose a well-substantiated set of parameters. It should be noted that the use of the MOMD and SRLS models in recent studies<sup>17,18,20</sup> also had not led to good quantitative reproduction of experimental results. The problem of unambiguous determination of the best fit parameters has not been discussed in the literature since no studies were reported in which characteristic times of rotation and the cage potential were varied simultaneously.

In our opinion, the fact that the use of the MOMD model proved negative can be explained as follows.

1. The parameters describing the times of rotation of the probe inside the cage, as well as the parameters of the cage potential, characterize restricted and anisotropic intracage motions. These two sets of parameters are not independent. This is the reason for ambiguity of the results of simulation where nearly the same simulated spectra correspond to different sets of parameters.

2. In the known models, the cage potential is represented by the first two or four terms of the expansion in spherical functions and is therefore described by harmonic functions. Actual interaction between the probe molecule and matrix cage and the formation of a complex are analogous in nature. Characteristic of such specific interactions is a strong orientational dependence, which can be adequately described only using a very large set of harmonic functions (a large number of terms of the expansion in spherical functions). Because of the simple analytical form of the potential used in the MOMD and SRLS models, experimental spectra cannot be well simulated in the temperature interval corresponding to passage from intracage motion to rotation in isotropic medium.

In temperature range V ( $T > 303$  K), we obtained satisfactory results by simulating the ESR spectra using the model of isotropic Brownian diffusion. The activation energy of the probe rotation in glycerol,  $E_a = 12.5$  kcal mol<sup>-1</sup>, determined from the temperature dependence of the diffusion coefficient plotted in the Arrhenius coordinates is close to that obtained previously for deuterated TEMPON radical in glycerol- $d_8(85\%)$ -D<sub>2</sub>O mixture (15 kcal mol<sup>-1</sup>).<sup>30</sup> Thus, the model of simple Brownian rotational diffusion appeared to be applicable to description of the ESR spectra in glycerol at temperatures above its melting temperature (18 °C). The analogous conclusion that this model works well only at temperatures above the melting temperature of the matrix was drawn<sup>19</sup> on the basis of quantitative simulation of the pattern of high-frequency (250 GHz) ESR spectra of nitroxyl probes in glassy *o*-terphenyl.

Temperature dependences of ESR spectra of the probe in polymer matrices are somewhat simpler. Quasibrations accompanied by gradual increase in the amplitude of angular displacements manifest themselves

in the spectra even at lowest temperatures (between 77 and 163 K for polystyrene and polyvinylbutyral) (see Fig. 4). This temperature interval is analogous to temperature range III in the case of glycerol matrix. Temperature variations of  $\langle \sin^2 \alpha_z \rangle$ ,  $\langle \sin^2 \alpha_y \rangle$ , and  $\langle \sin^2 \alpha_x \rangle$  values as well as their maximum values reached at 163 K are analogous to those observed in the glycerol matrix. No rotational motions about the  $x$  axis occur, as is the case of glycerol matrix. At  $T > 333$  K, the temperature dependences of the ESR spectra in polymer matrices are satisfactorily described in the framework of the model of strongly anisotropic rotation.<sup>8</sup> The rotational correlation times are listed in Table 3. As can be seen, no motion about the  $x$  axis of the radical occurs also under these conditions ( $\tau_c > 10^{-6}$  s). Temperature dependences of the characteristic times of rotation about the  $x$  and  $z$  axes exhibit strongly different activation energies. Thus, even near  $T_g$  of the polymer, the rotational mobility of the probe is determined by specific interactions with the medium.

We failed to obtain satisfactory results by simulating the ESR spectra over a wide temperature range (163 <  $T$  < 333 K) between the region of quasibrillations and that of true rotational motions in the polymer matrix using the known models. This temperature interval is similar to temperature range IV in the case of glycerol matrix, which was discussed above.

It is noteworthy that the temperature intervals determined using characteristic ESR spectra in polymer matrices are appreciably shifted toward lower temperatures as compared to glycerol matrix. This indicates a much closer packing of the molecules of glassy and liquid glycerol compared to that of the macromolecules of polymers.

**Table 3.** Temperature dependence of the tensor of the diffusion coefficient of TEMPON radical in polymer matrices, assessed using the model of anisotropic rotation

| T/K              | $R/s^{-1}$        |                   |
|------------------|-------------------|-------------------|
|                  | $y$               | $z$               |
| Polystyrene      |                   |                   |
| 333              | $4.30 \cdot 10^8$ | $1.06 \cdot 10^8$ |
| 343              | $4.19 \cdot 10^8$ | $1.30 \cdot 10^8$ |
| 353              | $4.57 \cdot 10^8$ | $1.13 \cdot 10^8$ |
| 363              | $5.15 \cdot 10^8$ | $1.16 \cdot 10^8$ |
| 373              | $5.57 \cdot 10^8$ | $1.14 \cdot 10^8$ |
| Polyvinylbutyral |                   |                   |
| 333              | $1.63 \cdot 10^8$ | $8.1 \cdot 10^7$  |
| 343              | $2.52 \cdot 10^8$ | $8.5 \cdot 10^7$  |
| 363              | $7.69 \cdot 10^8$ | $8.9 \cdot 10^7$  |

*Note.* The  $R_x$  value was not varied; dispersions of  $R_x$  and  $R_z$  values were no greater than  $1 \cdot 10^6$  s<sup>-1</sup>.

Thus, correspondence between experimental and simulated ESR spectra, which is characterized by the minimum of the sum of the squares of deviations between them, provides a rather rigorous criterion for adequacy of the chosen model of rotational diffusion.

Models of simple Brownian rotational diffusion can be used for quantitative description of the temperature dependence of the ESR spectra only in studying behavior of the probes in conventional liquids at temperatures above their melting temperatures. The model of isotropic Brownian diffusion is inapplicable to glassy polymers at  $T < T_g$ . In this case, the rotational correlation times of probe molecules in the polymer matrices obviously cannot likely be referred to any real physical process.

The ESR spectra of probe molecules in glassy media can be quantitatively simulated in the low-temperature range using the model of quasibrillations. It is also possible to obtain satisfactory results when simulating the spectra recorded at relatively high temperatures, namely, near the melting temperature of a low-molecular-weight glass and near the glass transition temperature of a polymer.

Quantitative simulation of the ESR spectra recorded at intermediate temperatures (at which both the intracage motions and rearrangement of the matrix cage occur) using the known models failed. The MOMD and SMLS models are not far enough advanced to offer a solution of this problem.

This work was financially supported by the Russian Foundation for Basic Research (Project No. 98-03-33161), the Ministry of Education of the Russian Federation (the Higher School Scientific Program 4.2 "Chemistry," Section "Theoretical and Applied Photochemistry. Kinetics and Mechanisms of Photochemical Processes in Complex Systems in Condensed Phase"), and the "Integration" Federal Program (Grant No. K0093).

## References

1. S. A. Zager and J. H. Freed, *J. Chem Phys.*, 1982, **77**, 2244.
2. N. N. Korst, A. N. Kuznetsov, A. V. Lazarev, and E. P. Gordeev, *Teor. Eksp. Khim.*, 1972, **8**, 63 [*Theor. Exp. Chem.*, 1972, **8** (Engl. Transl.)].
3. E. Meirovitch, D. Ignier, E. Ignier, G. Moro, and J. H. Freed, *J. Chem Phys.*, 1982, **77**, 3915.
4. L. J. Berliner, in *Biological Magnetic Resonance*, Ed. J. Reuben, Plenum, New York, 1989, **8**.
5. P. L. Kumler, *Methods Exp. Phys.*, 1980, **16(A)**, 442.
6. J. Bartos and Z. Hlouskava, *Polymer*, 1993, **34**, 4570.
7. P. Tormala, *J. Macromol. Sci., Rev. Macromol. Chem.*, 1979, **C17(2)**, 297.
8. A. M. Vasserman and A. L. Kovarskii, *Spinovye metki i zondy v fiziko-khimii polimerov* [*Spin Labels and Probes in Physicochemistry of Polymers*], Nauka, Moscow, 1986, 244 pp. (in Russian).
9. J. H. Freed, in *Spin Labelling: Theory and Application*, Ed. L. Berliner, Academic Press, New York, 1976, 640.
10. A. A. Dubinskii, G. G. Maresch, and H. W. Spiess, *J. Chem. Phys.*, 1994, **100**, 2437.



11. J. W. Saalmueller, H. W. Long, T. Volkmer, U. Wiesner, G. G. Maresch, and H. W. Spiess, *J. Pol. Sci., Pt. B: Pol. Phys.*, 1996, **34**, 1093.
12. S. A. Dzuba and Yu. D. Tsvetkov, *Chem. Phys. Lett.*, 1992, **188**(3-4), 217.
13. S. A. Dzuba, *Pure and Appl. Chem.*, 1992, **64**, 825.
14. S. A. Dzuba, *Phys. Lett.*, 1996, **A213**, 77.
15. S. V. Paschenko, S. A. Dzuba, A. Kh. Vorobiev, Yu. V. Toropov, and Yu. D. Tsvetkov, *J. Chem. Phys.*, 1999, **110**, 8150.
16. A. Kh. Vorobiev, V. S. Gurman, and T. A. Klimenko, *J. Phys. Chem., Chem. Phys.*, 2000, **2**, 379.
17. A. Polimeno and J. H. Freed, *J. Phys. Chem.*, 1995, **99**, 10995.
18. A. Polimeno, G. J. Moro, and J. H. Freed, *J. Chem. Phys.*, 1995, **102**, 8094.
19. K. A. Earle, L. K. Moscicki, A. Polimeno, and J. H. Freed, *J. Chem. Phys.*, 1997, **106**, 9996.
20. D. Xu, R. H. Crepeau, Ch. K. Ober, and J. H. Freed, *J. Phys. Chem.*, 1996, **100**, 15873.
21. E. Meirovitch, A. Nayeem, and J. H. Freed, *J. Phys. Chem.*, 1984, **88**, 3454.
22. E. Meirovitch and J. H. Freed, *J. Phys. Chem.*, 1984, **88**, 4995.
23. A. M. Wasserman, T. N. Khazanovich, and V. A. Kasaikin, *Appl. Magn. Reson.*, 1996, **10**, 413.
24. A. M. Vasserman, Yu. A. Zakharova, M. V. Motyakin, and V. A. Kasaikin, *Kolloid. Zh.*, 1996, **58**, 453 [*Colloid. J.*, 1996, **58**, 431 (Engl. Transl.)].
25. J. E. Dennis, D. M. Gay, and R. E. Welsch, *Transactions on Mathematical Software*, 1981, **7**, 348.
26. J. E. Dennis, D. M. Gay, and R. E. Welsch, *Transactions on Mathematical Software*, 1981, **7**, 369.
27. Ya. S. Lebedev, O. Ya. Grinberg, and A. A. Dubinskii, in *Nitroksil'nye radikaly. Sintez, khimiya, prilozheniya* [*Nitroxyl Radicals. Synthesis, Chemistry, Applications*], Nauka, Moscow, 1987 (in Russian).
28. O. Ya. Grinberg, A. A. Dubinskii, V. F. Shuvalov, L. G. Oranskii, V. I. Kurochkin, and Ya. S. Lebedev, *Dokl. Akad. Nauk SSSR*, 1976, **230**, 884 [*Dokl. Chem.*, 1976 (Engl. Transl.)].
29. D. J. Schneider and J. H. Freed, *Biological Magnetic Resonance*, Ch. 1, **8**, Eds. L. J. Berliner and J. Reuben, Plenum Press, New York, 1989.
30. J. S. Hwang, R. Mason, L. P. Hwang, and J. H. Freed, *J. Phys. Chem.*, 1975, **79**, 489.
31. D. H. Rasmussen and A. P. Mackenzie, *J. Phys. Chem.*, 1971, **75**, 967.

Received July 9, 1999;  
in revised form December 20, 1999